Defect quantification with reference-free thermal contrast and artificial neural networks

Hernán D. Benítez[a], Clemente Ibarra-Castanedo[b]

AbdelHakim Bendada [b], Xavier Maldague [b]

Humberto Loaiza [a], Eduardo Caicedo [a]

[a] Universidad del Valle, School of Electrical Engineering, Calle 13 Cra 100 Cali,Colombia
[b] Université Laval, Computer Vision and Systems Laboratory, Québec City , G1K7P4, Québec

ABSTRACT

The Infrared Nondestructive Testing (IRNT) methods based on thermal contrast are strongly affected by non-uniform heating at the surface. Hence, the results obtained from these methods considerably depend on the chosen reference point. One of these methods is Artificial Neural Networks (ANN) that uses thermal contrast curves as input data for training and test in order to detect and estimate defect depth.

The Differential Absolute Contrast (DAC) has been successfully used as an alternative thermal contrast to eliminate the need of a reference point by defining the thermal contrast with respect to an *ideal* sound area. The DAC technique has been proven effective to inspect materials at early times since it is based on the 1D solution of the Fourier equation. A modified DAC version using thermal quadrupoles explicitly includes the sample thickness in the solution, extending in this way the range of validity when the heat front approaches the sample rear face.

We propose to use ANN to detect and quantify defects in composite materials using data extracted from the modified DAC with thermal quadrupoles in order to decrease the non-uniform heating and plate shape impact on the inspection.

Keywords: Artificial Neural Networks, Reference-free thermal contrast, Infrared nondestructive testing, Thermal quadrupoles

1. INTRODUCTION

Infrared nondestructive testing (IRNT) is a technique in which the specimen surface is thermally stimulated to produce a temperature difference between sound (free of defects) areas and eventual defective regions. It is well known that thermal contrast-based quantification methods are strongly affected by the non-uniform heating, the sample shape and the chosen sound area.

In previous works, Artificial Neural Networks (ANN) were used for defect detection and quantification. Different kinds of data have been proposed to train and test the ANN, for instances: raw temperature and time derivatives,[1,2] TSR (Thermal Signal Reconstruction) polynomial fitting coefficients,[3] phase and phase contrast[4,5] and thermal contrast.[6–8] The thermal contrast approach allows evaluating defect visibility and enhancing image quality. However, the ANN defect detection and quantification is strongly affected by the selected reference sound area.

The differentiated absolute contrast (DAC) method was developed to perform a more convenient computation of the sound area temperature through the 1D solution of the Fourier equation for homogeneous and semi-infinite materials stimulated with a heat Dirac pulse[9,10] described by Eq.1:

$$\Delta T_{DAC} = T(t) - \sqrt{\frac{t'}{t}} T(t') \tag{1}$$

Further author information: Escuela de Ingeniería Eléctrica y Electrónica Universidad del Valle Calle 13 Cra 100 Cali, Colombia. E-mail: hbenitez@univalle.edu.co, Telephone: + 57 2 3391780, ext 116

Thermosense XXIX, edited by Kathryn M. Knettel, Vladimir P. Vavilov, Jonathan J. Miles,
Proc. of SPIE Vol. 6541, 65410V, (2007) · 0277-786X/07/$18 · doi: 10.1117/12.718272

where T is temperature, t' is a given value of time t ranging between the time of flash pulse and the time at which the first defect becomes visible. This model does not include the sample thickness therefore the DAC accuracy decreases for long times after heating when the heat front reaches the sample face opposite to irradiation. In addition, strictly speaking, this approach is only valid for the case of shallow defects and/or thick samples. A modified DAC version in which the sample thickness is explicitly introduced by using the thermal quadrupoles theory allows the extension of the range of validity.

This paper shows the application of ANN for the detection and characterization of defects in composite samples affected by non-uniform heating or with complex shape. The training and validation data are theoretical and experimental thermal curves processed with the improved DAC version.

The rest of the paper is organized as follows: Section 2 describes the modified DAC deduction by using thermal quadrupoles. Section 3 presents the training and validation of the neural system with synthetical and experimental data.

2. MODIFIED DAC VERSION DEFINITION

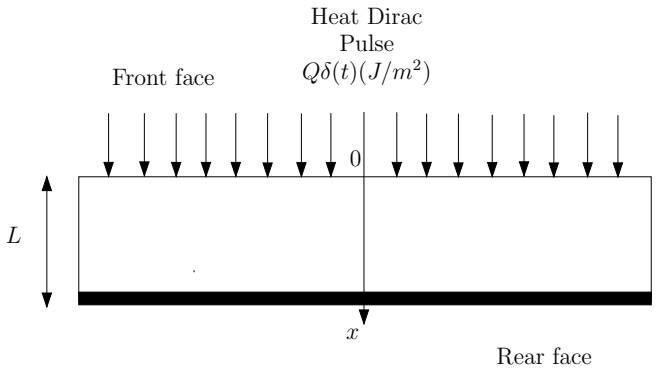

Figure 1. Limited thickness plate excited with a heat Dirac pulse

Figure 1 shows a plate with thickness $L(m)$ whose front face ($x = 0$) is excited with a heat Dirac pulse with energy density $Q(J/m^2)$ while its rear face ($x = L$) is thermically isolated.

The temperature Θ in Laplace domain on its front face is given by Equation (2)[11]

$$\Theta = \frac{Q}{b} \frac{coth\sqrt{\frac{pL^2}{\alpha}}}{\sqrt{p}} \tag{2}$$

where b is thermal effusivity, α is thermal diffusivity and p is the Laplace variable.

Now the modified DAC deduction will be explained. The temperature in the time domain at times t and t' can be found by using the inverse Laplace transform[12]:

$$T(t) = \frac{Q}{b} L^{-1} \left[\frac{coth\sqrt{\frac{pL^2}{\alpha}}}{\sqrt{p}} \right] \Bigg|_t \tag{3}$$

$$T(t') = \frac{Q}{b} L^{-1} \left[\frac{coth\sqrt{\frac{pL^2}{\alpha}}}{\sqrt{p}} \right] \Bigg|_{t'} \tag{4}$$

From Eq.4 we can derive that

$$\frac{Q}{b} = \frac{T(t')}{L^{-1} \left[\frac{coth\sqrt{\frac{pL^2}{\alpha}}}{\sqrt{p}} \right] \Big|_{t'}} \tag{5}$$

Replacing Eq. 5 in Eq. 3 we get:

$$\frac{T(t)}{T(t')} = \frac{L^{-1} \left[\frac{coth\sqrt{\frac{pL^2}{\alpha}}}{\sqrt{p}} \right] \Big|_t}{L^{-1} \left[\frac{coth\sqrt{\frac{pL^2}{\alpha}}}{\sqrt{p}} \right] \Big|_{t'}} \tag{6}$$

$$\Delta T_{DACcorr} = T(t) - \frac{L^{-1} \left[\frac{coth\sqrt{\frac{pL^2}{\alpha}}}{\sqrt{p}} \right] \Big|_t}{L^{-1} \left[\frac{coth\sqrt{\frac{pL^2}{\alpha}}}{\sqrt{p}} \right] \Big|_{t'}} T(t') \tag{7}$$

The corrected DAC in Eq. 7 explicitly contains the specimen thickness L and does not depend on the energy density Q. In this section we explained the methodology to deduce the corrected DAC, the next section shows the procedure followed to train and validate the neural networks in order to estimate defect depth in composite samples affected by non-uniform heating and with complex shapes.

3. VALIDATION WITH SYNTHETIC AND EXPERIMENTAL DATA

Modified DAC data curves obtained from synthetic and experimental temperature curves will be used in this section for training and validation of ANN. ANN are known by their ability to perform a non linear mapping between two sets of variables,[13] their low sensitivity to noise and capabilities for learning and generalization.[14, 15] In this study we are only interested in multi-layer perceptron networks (MLP) which are supervised networks. The MLP network is trained using the back propagation (Levenberg-Marquardt optimization) algorithm which is probably the most used learning algorithm used in the recent years.

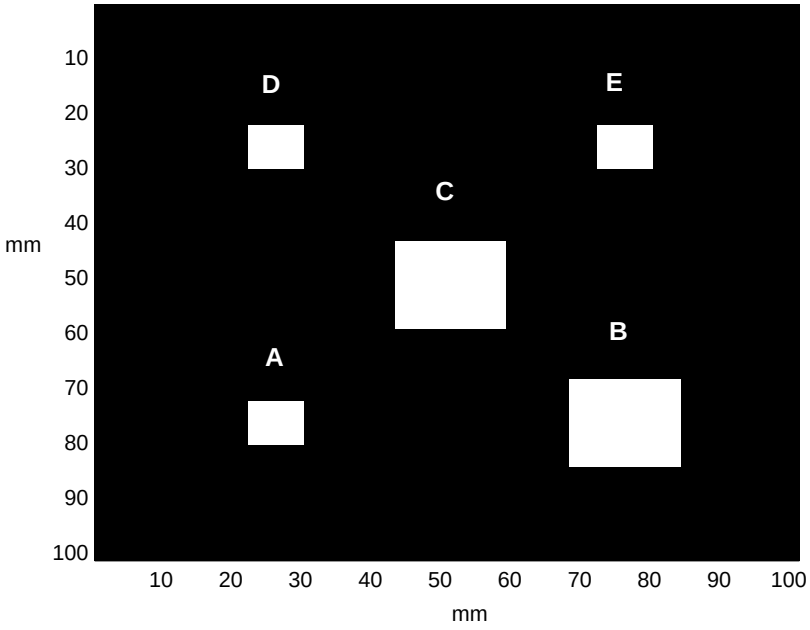

Figure 2. Defect distribution on CFRP sample

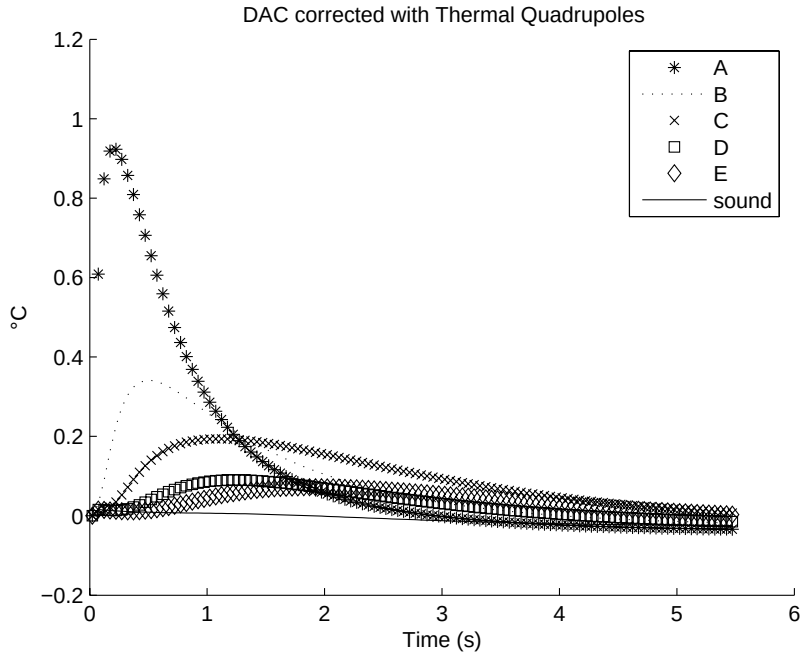

Figure 3. Modified DAC curves for defects A,B,C,D and E with depths 0.2,0.4,0.6,0.8 and 1.0 mm

3.1. Synthetic data

Simulated carbon fiber reinforced plastic (CFRP) samples with air delaminations were designed using *ThermoCalc6L* software from *Innovations Inc*[16] in order to generate the synthetic temperature curves. The plate has a thickness of 2 mm and lateral dimensions (L_1 and L_2) of 100 mm. There are two sizes of defects whose

dimensions are 8 mm x 8 mm x 0.1 mm (A,D,E) and 16 mm x 16 mm x 0.1 mm (B,C). Figure 2 shows the defect distribution on CFRP plate and Figure 3 presents the curves of the modified DAC on the center of every defect.

After several tests we settled for a 30 x 5 x 6 defect depth estimator network. This was trained with 1200 input-output pairs. In this training set 600 curves correspond to defective pixels and 600 curves to sound pixels. The defects depths used for training ranges from 0.1 to 1.5 mm in increments of 0.1 mm so that every defect depth is represented by 40 modified DAC curves. This training set was generated using every point in the modified DAC curves as means of 40 normal probabilistic distributions with $\sigma = 0.025$, this value of σ was estimated according to the procedure described in Ref. 17 to characterize IR camera noise standard deviation. In this case the characterized camera is a Santa Barbara FPA which is used for the acquisition of the experimental data.

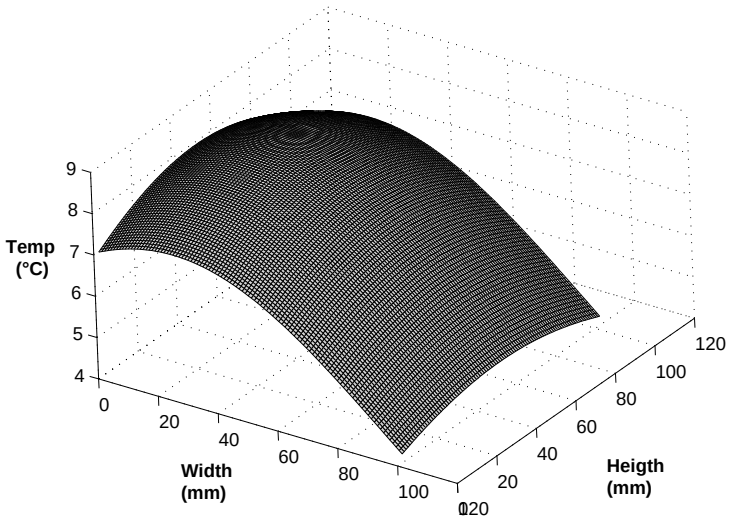

Figure 4. Non uniform heating pattern applied to the validation samples

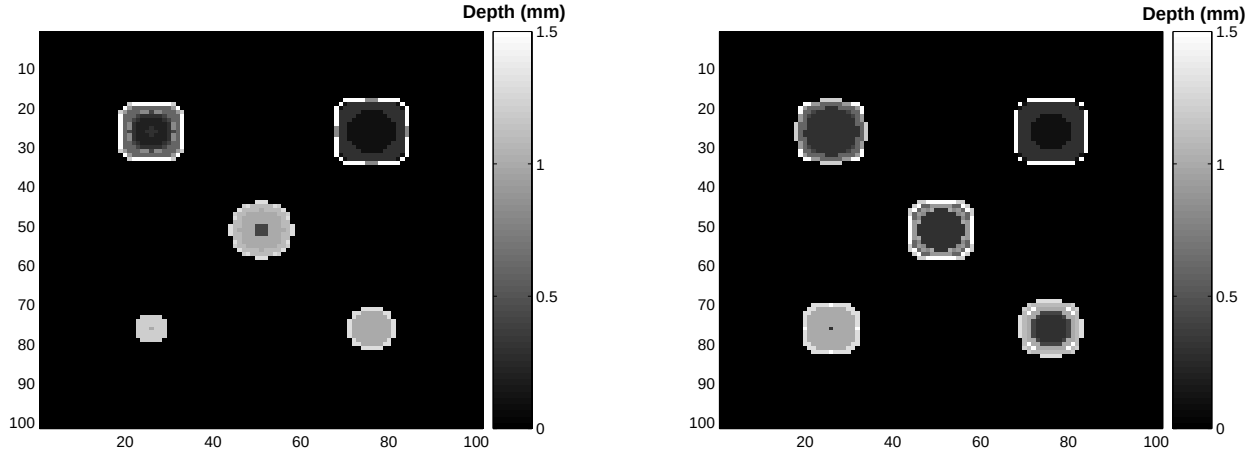

(a) (b)

Figure 5. (a) Result of ANN for defects (A,B,C,D,E) at depths (a) 1.5, 1.4, 1.3, 1.2, 1.1 mm (b) 1.0, 0.9, 0.8, 0.7 0.6 mm

Figure 5 shows the validation results of the trained ANN with 2 CFRP plates affected by non-uniform heating

as indicated in Figure 4 by the surface of the first thermogram after heating. It is observed that the highest error are presented at defect edges, this is due to the fact that thermal contrast in the pixels at defect edges is low compare to those at the defect center therefore these pixels have a highest probability of being erroneuosly classified by the network. However, in spite of the uneven heating the network was able to detect the defects in every sample although it was not able to estimate its depth properly.

3.2. Experimental data

To generate training data twelve (12) experiments were carried out on a sample with 25 defects so that every defect had twelve observations producing 300 curves from defective pixels and 300 from sound pixels to complete 600 observations for the training set. These experiments were performed using two photographic flashes (Balcar FX 60, 6.4 kJ), with a 5 ms pulse as the excitation source. All the thermogram sequences were recorded using a FPA infrared camera (Santa Barbara Focalplane SBF125, 3 to 5 μ m), with a 320 x 256 pixel array. The specimens used for network training and validation are made of CFRP. The training specimen is planar as shown in Figure 6 and the validation specimen has curved shapes as illustrated in Figure 7. In each CFRP specimen, twenty-five (25) square TeflonTM insertions of different sizes were placed between plies at different locations as indicated. The thickness for each specimen is 2 mm.

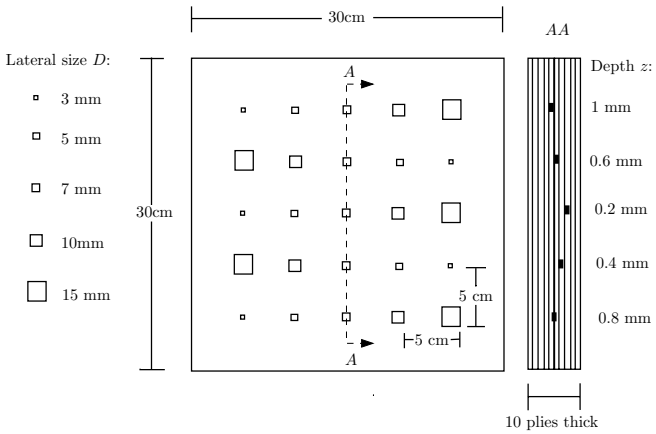

Figure 6. Configuration of training CFRP sample

Figures 8 and 9 present the corrected DAC curves for inserts with diameter $D = 15$ mm in the training and validation sample. For defect characterization in this case two neural networks were used. The first stage is used to detect the defects and the second stage is used to estimate the depth of those pixels classified as defective by the detector network. After several tests we settled for a 33 x 10 x 1 defect detection network and for 33 x 5 x 6 defect depth estimation network. Figure 10(a) shows the real defect map of the validation sample and 10(b) presents the defect depth map estimated by the neural system after applying a 2D median filter with kernel size 4 x 4. In both cases the color scale represents the defect depth. The neural system correctly classified the 98 % of the non defective pixels and the 76% of the defective pixels. It is important to note that in spite of the curved shape of the validation sample the neural sytem detected the defects with depth 0.8 mm. However, this was not the case for the defects with 1 mm of depth since the thermal contrast curves for this depth resembles the thermal contrast curves of the sound pixels.

4. CONCLUSIONS

ANN were trained with reference-free thermal contrast curves and tested with composite materials in order to carry out depth estimation of ribbon like delaminations in CFRP. The advantage of this approach is that the difference between sound and defective areas is enhanced and that the need of selecting a non defective area is eliminated. Here ANN essentially perform a classification of the input patterns, which are modified DAC profiles of the pixels in the thermographic image sequence. For the experimental data the classification is done

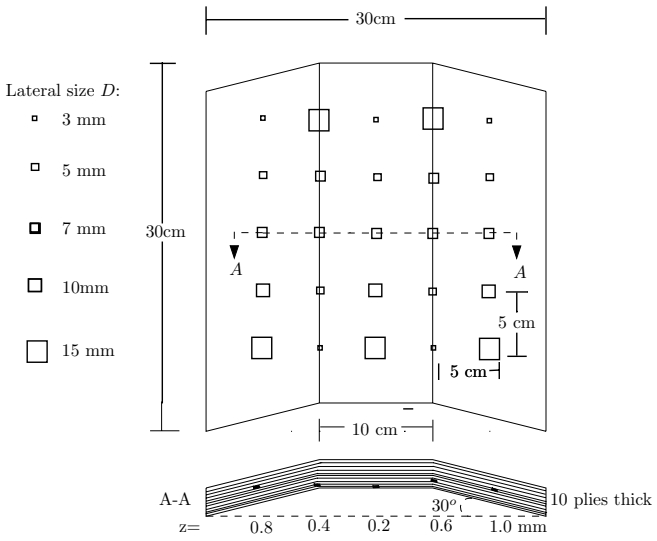

Figure 7. Configuration of validation CFRP sample

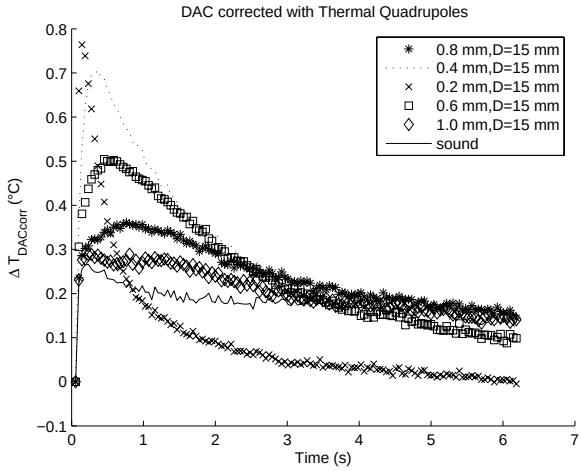

Figure 8. Modified DAC curves for the five largest defects at different depths (15 mm in lateral size) in training sample

in a two step approach, first the defective pixels are detected and then they are classified in one of the possible depths. This combined approach allows the reduction of false defect detection since every network is specialized in a different type of data set. On the other hand, synthetical and experimental data showed that non-uniform heating and complex shape have little impact on depth inversion results.

Finally, the disadvantage of using ANN in IRNDT is that it requires at least a specimen with a set of known defects to provide the information required for the ANN training and it can then be only used with the same material and acquisition system.

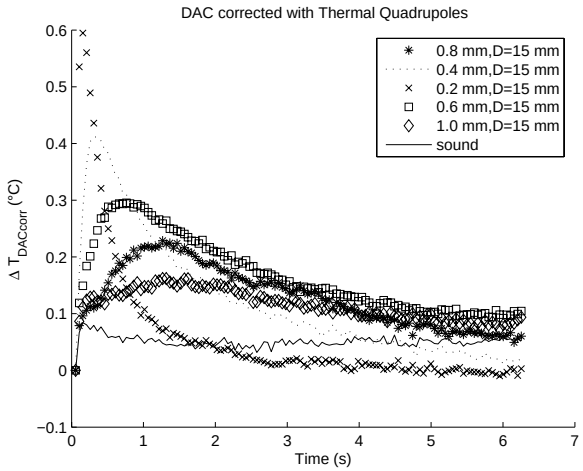

Figure 9. Modified DAC curves for the five largest defects at different depths (15 mm in lateral size) in validation sample

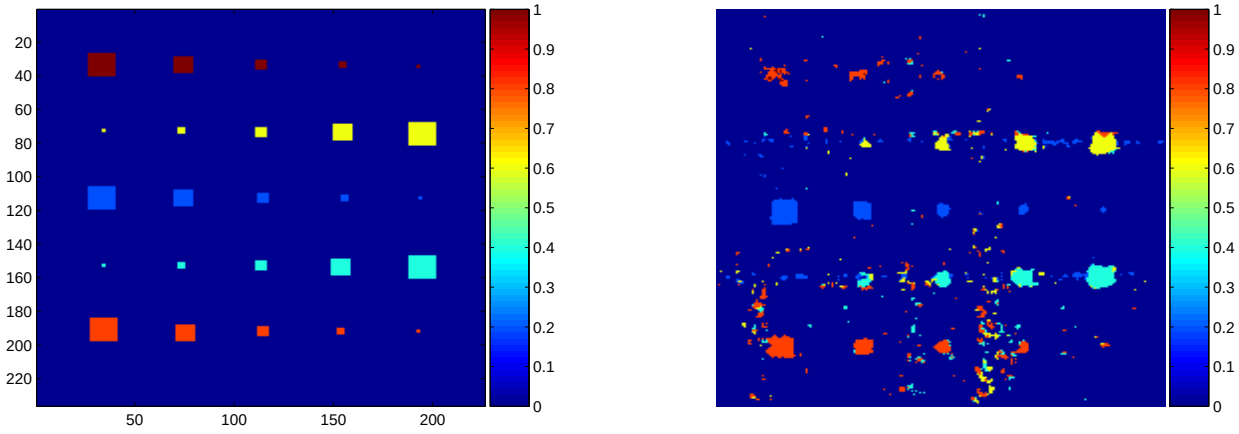

(a) (b)

Figure 10. Defect depth map: (a)Real (b)Estimated

ACKNOWLEDGMENTS

Special acknowledgment for financial support is extended to the Colombian Institute of Science and Technology COLCIENCIAS and Universidad del Valle.

REFERENCES

1. D. R. Prabhu and W. Winfree, "Neural network based processing of thermal NDE data for corrosion detection," *Review of progress in quantitative nondestructive evaluation* **12**, 1993.
2. H. Trétout, D.David, J.Marin, Y.Dissenter, M.Court, and M.Avenas-Payan, "An evaluation of artificial neural networks applied to infrared thermograph inspection of composite aerospace structures," *Review of Progress in Quantitative Nondestructive Evaluation Editor D.O Thompson and D.E Chimenti* **14A**, pp. 827–834, 1995.
3. H. Benítez, C. Ibarra-Castanedo, H. Loaiza, E. Caicedo, A. Bendada, and X. Maldague, "Defect quantification with thermographic signal reconstruction and artificial neural networks," *Proceedings of 8th Conference on Quantitative Infrared Thermography, Padova, Italy* , 2006.

4. X. Maldague, Y. Largouet, and J. Couturier, "Depth study in pulse phase thermography using neural networks: modelling, noise, experiments," *Revue Générale de Thermique* **37**, pp. 704–708, 1998.
5. S. Vallerand and X. Maldague, "Defect characterization in pulsed thermography : a statistical method compared with kohonen and perceptron neural networks," *NDT & E International* **37**(5), 2000.
6. A.Darabi and X. Maldague, "Neural network based defect detection and depth estimation in TNDE," *NDT & E International* **35**(3), 2002.
7. P. Bison, C. Bressan, R. D. Sarno, E. Grinzato, S. Marinetti, and G. Manduchi, "Thermal NDE of delaminations in plastic materials by neural network processing," *QIRT 94-Eurotherm Series 42 EETI ed,Paris* , 1996.
8. P. Bison, S. Marinetti, G. Manduchi, and E. Grinzato, "Improvement of neural networks performances in thermal NDE," *Advances in Signal Processing for Nondestructive Evaluation of Materials,3rd Quebec Workshop(1997),Quebec City, American Society of Nondestructive Testing Press,uppercaseTONES ,221-227* , 1998.
9. M. Pilla, M. Klein, X. Maldague, and A. Salerno, "New absolute contrast for pulsed thermography," *Proceddings. 6th Conference on Quantitative Infrared Thermography, Eds. D. Balageas, G. Busse, G.M. Carlomagno, and S. Svaic, Univ. of Zagreb, Croatia* , pp. 53–58, 2002.
10. D. González, C. Ibarra-Castanedo, M. Pilla, M. Klein, J. M. López-Higuera, and X. Maldague, "Automatic interpolated differentiated absolute contrast algorithm for the analysis of pulsed thermographic sequence," *Proceedings 7th Conference on Quantitative Infrared Thermography, Eds. D. Balageas, G. Busse, G.M. Carlomagno, and J.-M. Buchlin, von Karman Institute, Rhode Saint Gense, Belgium,* , pp. H.16.1–H.16.6, 2004.
11. D. Maillet, S. André, J. Batsale, A. Degiovanni, and C. Moyne, *Thermal quadrupoles: solving the heat equation through integral transforms*, John Wiley and Sons, USA.
12. H. Stehfest, "Remarks on algorithm 368: Numerical inversion of laplace transforms," *Communications of the A.C.M* **13**(1), pp. 47–49, 1970.
13. C. Bishop, "Neural networks and their applications," *Rev.Sci.Instrum* **65**(6), 1994.
14. M. Saintey and D. Almond, "An artificial neural network interpreter for transient thermography image data," *NDT & E International* **30**(5), 1997.
15. G. Manduchi, S.Marinetti, P. Bison, and E. Grinzato, "Application of neural network computing to thermal non-destructive," *Neural Comput & Applic* **6**, pp. 148–157, 1997.
16. V.Vavilov, "Three dimensional analysis of transient thermal NDT problems by data simulation and processing," *Thermosense XXII Proceedings SPIE* **4020**, 2000.
17. S. Marinetti, X.Maldague, and M.Prystay, "Calibration procedure for focal plane array cameras and noise equivalent material loss for quantitative thermographic NDT," *Materials Evaluation* **55**(3), 1997.